



# **Aluminum and bone: Review of new clinical circumstances associated with Al(3+) deposition in the calcified matrix of bone**

Daniel Chappard, Pascal Bizot, Guillaume Mabilieu, Laurent Hubert

## **► To cite this version:**

Daniel Chappard, Pascal Bizot, Guillaume Mabilieu, Laurent Hubert. Aluminum and bone: Review of new clinical circumstances associated with Al(3+) deposition in the calcified matrix of bone. *Morphologie*, 2016, 100 (329), pp.95-105. <10.1016/j.morpho.2015.12.001>. <hal-01392262>

**HAL Id: hal-01392262**

**<https://hal.science/hal-01392262v1>**

Submitted on 14 Oct 2021

**HAL** is a multi-disciplinary open access archive for the deposit and dissemination of scientific research documents, whether they are published or not. The documents may come from teaching and research institutions in France or abroad, or from public or private research centers.

L'archive ouverte pluridisciplinaire **HAL**, est destinée au dépôt et à la diffusion de documents scientifiques de niveau recherche, publiés ou non, émanant des établissements d'enseignement et de recherche français ou étrangers, des laboratoires publics ou privés.



Distributed under a Creative Commons CC BY 4.0 - Attribution - International License

# Aluminum and bone: Review of new clinical circumstances associated with Al<sup>3+</sup> deposition in the calcified matrix of bone

*Aluminium et os : revue de nouvelles circonstances cliniques où Al<sup>3+</sup> peut être localisé dans la matrice osseuse*

D. Chappard<sup>a,b,\*</sup>, P. Bizot<sup>c</sup>, G. Mabillean<sup>a,b</sup>, L. Hubert<sup>c</sup>

<sup>a</sup> Groupe études remodelage osseux et biomatériaux (GEROM), LHEA, IRIS-IBS institut de biologie en santé, CHU d'Angers, LUNAM université Nantes Angers Le Mans, 49933 Angers cedex, France

<sup>b</sup> Service commun d'imagerie et analyses microscopiques (SCIAM), IRIS-IBS institut de biologie en santé, CHU d'Angers, LUNAM université, 49933 Angers cedex, France

<sup>c</sup> Département de chirurgie osseuse, CHU d'Angers, 49933 Angers cedex, France

## KEYWORDS

Aluminum;  
Bone;  
Mineralization;  
Biomaterial;  
Titanium;  
TA6V;  
Metal oxidation;  
Exostosis;  
Metal toxicity

**Summary** Several decades ago, aluminum encephalopathy associated with osteomalacia has been recognized as the major complication of chronic renal failure in dialyzed patients. Removal of aluminum from the dialysate has led to a disappearance of the disease. However, aluminum deposit occurs in the hydroxyapatite of the bone matrix in some clinical circumstances that are presented in this review. We have encountered aluminum in bone in patients with an increased intestinal permeability (coeliac disease), or in the case of prolonged administration of aluminum anti-acid drugs. A colocalisation of aluminum with iron was also noted in cases of hemochromatosis and sickle cell anemia. Aluminium was also identified in a series of patients with exostosis, a frequent benign bone tumor. Corrosion of prosthetic implants composed of grade V titanium (TA6V is an alloy containing 6% aluminum and 4% vanadium) was also observed in a series of hip or knee revisions. Aluminum can be identified in undecalcified bone matrix stained by solochrome azurine, a highly specific stain allowing the detection of 0.03 atomic %. Colocalization of aluminum and iron does not seem to be the fruit of chance but the cellular and molecular mechanisms are still poorly understood. Histochemistry is superior to spectroscopic analyses (EDS and WDS in scanning electron microscopy).

\* Corresponding author. Groupe études remodelage osseux et biomatériaux (GEROM), LHEA, IRIS-IBS institut de biologie en santé, CHU d'Angers, LUNAM université Nantes Angers Le Mans, 49933 Angers cedex, France.

E-mail address: daniel.chappard@univ-angers.fr (D. Chappard).

## MOTS CLÉS

Aluminium ;  
Tissu osseux ;  
Minéralisation ;  
Biomatériaux ;  
Titane ;  
TA6V ;  
Oxydation  
métallique ;  
Exostose ;  
Toxicité des métaux

**Résumé** L'encéphalopathie aluminique associée à une ostéomalacie a été reconnue il y a plusieurs décennies comme une complication majeure de l'insuffisance rénale chronique chez les patients dialysés. L'élimination de l'aluminium des bains de dialyse a conduit à la disparition de cette maladie. Cependant, des dépôts d'aluminium peuvent survenir dans l'hydroxyapatite de la matrice osseuse au cours de nouvelles circonstances cliniques qui sont décrites dans cette revue. Nous avons observé de l'aluminium dans l'os de patients qui présentaient une perméabilité intestinale accrue (maladie coeliaque) ou en cas d'administration prolongée de médicaments anti-acides contenant de l'aluminium. Une colocalisation de l'aluminium et du fer est aussi rencontrée dans les cas d'hémochromatose et de drépanocytose. La corrosion des implants prothétiques orthopédiques composés de titane de grade V (TA6V – un alliage contenant 6 % d'aluminium et 4 % de vanadium), a aussi été observée dans une série de prothèses de hanche ou de genou après révision prothétique. L'aluminium a aussi été identifié dans une série de patients jeunes avec exostose, une tumeur osseuse bénigne. L'aluminium peut être identifié dans la matrice osseuse non décalcifiée par la coloration au solochrome azurine, un colorant hautement spécifique qui permet la détection de 0,03 % d'aluminium en fraction atomique. La colocalisation de l'aluminium et du fer ne semble pas être le fruit du hasard mais les mécanismes cellulaires et moléculaires d'entrée de l'aluminium et du fer dans la cellule sont encore mal connus. L'histochimie apparaît comme une méthode supérieure aux analyses spectroscopiques (EDS et WDS) couplées à la microscopie électronique à balayage.

## Introduction

Bone matrix is composed of two phases:

- an organic phase is elaborated by osteoblasts and is mainly composed of type I collagen microfibrils and non-collagenous proteins;

- a mineral phase which is composed of numerous hydroxyapatite crystals (HA) deposited between the collagen microfibrils (Fig. 1).

The formula for biological HA is  $\text{Ca}_{10}(\text{PO}_4)_6(\text{OH})_2$ . In mature bone, nucleation of the HA crystals seems to be due to non-collagenous proteins such as the bone sialoprotein (BSP) deposited at the mineralization front

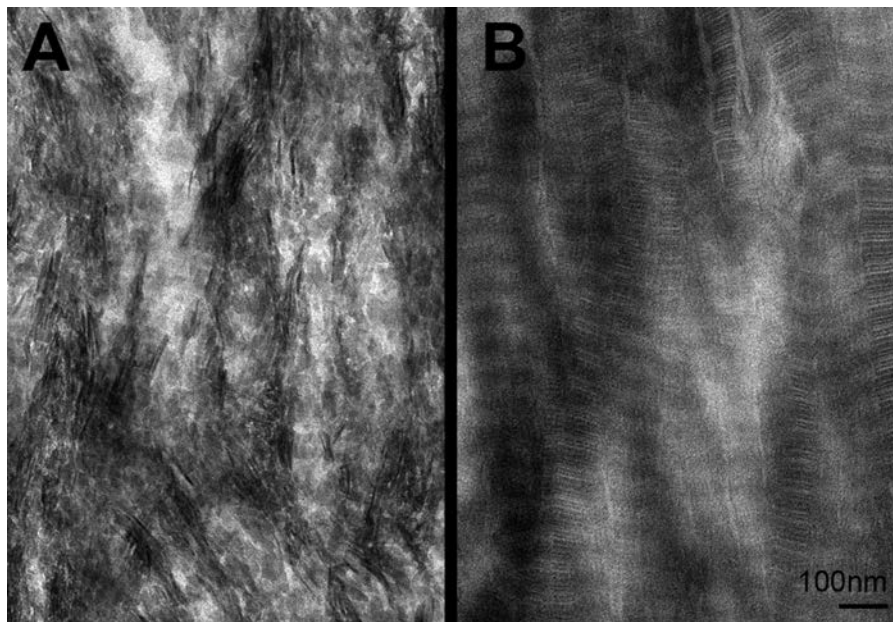


**Figure 1** Transmission electron microscopy of the bone matrix. A) Undecalcified ultrathin section showing the mineral phase composed of hydroxyapatite crystals in the form of tablets. B) After decalcification, the organic phase composed of collagen microfibrils is clearly unmasked.

*Microscopie électronique à transmission de la matrice osseuse. A) coupe ultra fine non décalcifiée montrant la phase minérale constituée de cristaux d'hydroxyapatite présents sous forme de tablettes. B) Après décalcification, la phase organique composée de microfibrilles de collagène est clairement démasquée.*

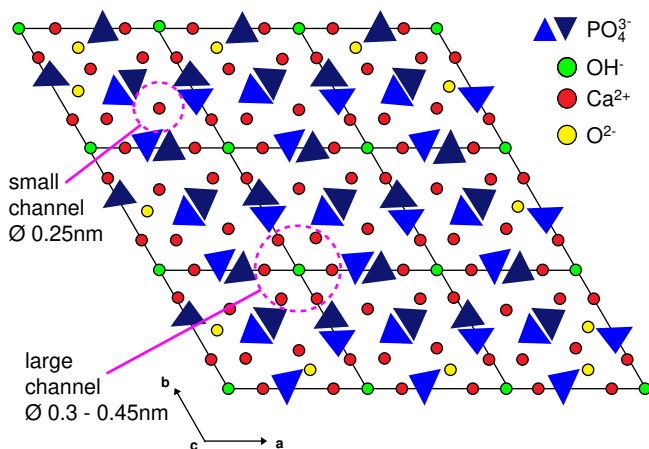


**Figure 2** Projection on the plane (001) of the crystallographic structure of hydroxyapatite with the localization of the small and large channels. The large channel, centered on an  $\text{OH}^-$  group and outlined by  $\text{PO}_4^{3-}$ , is the site for ionic substitutions. *Projection sur le plan (001) de la structure cristallographique de l'hydroxyapatite montrant la localisation des petits et grands tunnels. Le grand tunnel, centré sur un groupe  $\text{OH}^-$  est entouré par des  $\text{PO}_4^{3-}$ , il s'agit du site possible pour les substitutions anioniques.*

[1]. Alkaline phosphatase, elaborated and secreted by osteoblasts in the osteoid tissue (seams of recently synthesized organic bone matrix) allows the development of the mature HA crystals from the crystal nuclei. The enzyme substrates are pyridoxal phosphate, ATP, ADP, AMP, glucose-1-AMPC, glucose-6-phosphate, pyrophosphate and phosphor-ethanolamin present in the extracellular fluids [2]. Alkaline phosphatase also acts as a phosphate transporter to the mineralization front, allowing the accretion of phosphates on the calcium atoms of the HA crystal.

From a crystallographic point of view, the arrangement of  $\text{Ca}^{2+}$ ,  $\text{PO}_4^{3-}$  and  $\text{OH}^-$  groups in the crystal can be modeled as in Fig. 2 [3]. In this atomic lattice, two channels can be described: a small one (0.25 nm in diameter) and a large one (0.3–0.45 nm in diameter). In this large channel, a number of atom substitutions are possible. Hydroxide groups, for example, can be substituted by anions such as F; phosphate can be substituted by other anions (e.g. carbonate) and calcium can be replaced by metallic cations such as  $\text{Fe}^{3+}$ ,  $\text{Sr}^{2+}$ ,  $\text{Pb}^{2+}$ ... The non-exhaustive list of these substitutions appears on Table 1 [3]. Some of these substitutions ( $\text{F}^-$  and  $\text{Sr}^{2+}$ ) have been proposed in therapeutic for the treatment of osteoporosis (these drugs are non-longer used in clinical practice). It should be noted that any substitution changes the crystal properties (e.g.  $\text{F}^-$  increases acid resistance of HA to hydrolysis) with a consequence at the tissue level on the bone quality.

Histochemistry is a powerful tool to characterize mineralization of the bone matrix and to identify the presence of certain metal ions abnormally present in HA where they can alter bone quality. The Perls' staining is a worldwide admitted histochemical stain for iron. The method works on soft and hard tissues. In the presence of ferrocyanide ions,  $\text{Fe}^{3+}$  (but not  $\text{Fe}^{2+}$ ) is precipitated as a highly water-insoluble blue complex also termed Prussian blue. In bone, it

**Table 1** Non-exhaustive list of cationic (for  $\text{Ca}^{2+}$ ) and anionic substitutions (for  $\text{PO}_4^{3-}$  and  $\text{OH}^-$ ). The carbonate substitution of a phosphate is called  $\alpha$  substitution, and for a hydroxide, a  $\beta$  substitution.  $\beta$  substitution increases in the human bone matrix during ageing.

*Liste non exhaustive des substitutions cationiques (pour le  $\text{Ca}^{2+}$ ) et anioniques (pour  $\text{PO}_4^{3-}$  et  $\text{OH}^-$ ). La substitution des phosphates par les carbonates est appelée substitution  $\alpha$ , et un hydroxyl par un carbonate substitution  $\beta$ . La substitution  $\beta$  augmente au cours du vieillissement.*

$\text{Ca}^{2+}$			$\text{PO}_4^{3-}$			$\text{OH}^-$	
$\text{Pb}^{2+}$	$\text{Na}^+$	$\text{Fe}^{3+}$	$\text{VO}_4^{3-}$	$\text{CO}_3^{2-}$	$\text{SiO}_4^{4-}$	$\text{F}^-$	$\text{CO}_3^{2-}$
$\text{Cd}^{2+}$	$\text{Li}^+$	$\text{La}^{3+}$	$\text{AsO}_4^{3-}$	$\text{SO}_4^{2-}$	$\text{GeO}_4^{4-}$	$\text{Cl}^-$	$\text{O}^{2-}$
$\text{Zn}^{2+}$	$\text{K}^+$	$\text{Al}^{3+}$	$\text{MnO}_4^{3-}$	$\text{HPO}_4^{2-}$		$\text{I}^-$	$\text{S}^{2-}$
$\text{Ni}^{2+}$	$\text{Ag}^+$					$\text{Br}^-$	
$\text{Mn}^{2+}$							
$\text{Ba}^{2+}$							
$\text{Sr}^{2+}$							
$\text{Mg}^{2+}$		Lacuna					Lacuna

is preferable to avoid the use a counterstain dye if one wants to clearly identify the iron bands in the bone matrix [4–7].  $\text{Fe}^{3+}$  is deposited in the cement or arrest lines when a BSU is formed, either in cortical and/or trabecular bone. These lines are known to contain specific proteins (osteopontin and osteocalcin) that can bind metal ions. Decalcification of bone sections abolishes the staining because  $\text{Fe}^{3+}$  is bound to the HA crystals. It has been shown by a very sensitive method (micro X-ray fluorescence analysis with a synchrotron) that Zn and Pb ions which are also present in the interstitial fluid can accumulate in the cement lines by uptake in the HA crystal and attachment to these proteins [8].

Histochemical identification of aluminum in bone was extensively studied in patients with renal failure who developed encephalopathy and osteomalacia (see below). The different methods only work on undecalcified bone sections [9]. Aluminum can be stained by the aluminon technique using aurine tricarboxylic stain [4,10]. The method was found more sensitive than atomic absorption spectrometry [11]. Several authors have reported that the regressive staining with solochrome azurine B (also termed Mordant blue B or chrome azurol B - CI 43830) [12] gives better results and identifies more bands in the bone matrix [13–16]. We have found that spectroscopic methods such as scanning electron microscopy (SEM) coupled with X-ray energy dispersive spectroscopy (EDS) cannot identify aluminum and iron on bone samples due to the low concentration of these metals in the HA crystals. The limit of detection of EDS is 0.05% (atomic %) [17,18]. We have identified these metals by wavelength dispersive spectroscopy (WDS), coupled with SEM, and the local concentrations of these metals is in the range of 0.03–0.035% at a maximum [19]. However, this method does not allow mapping images of the tissues.

## In vitro models of calcification

A number of models have been described to mimic in vitro the calcification of the bone matrix. We have developed a synthetic polymer (poly (2-hydroxyethyl)

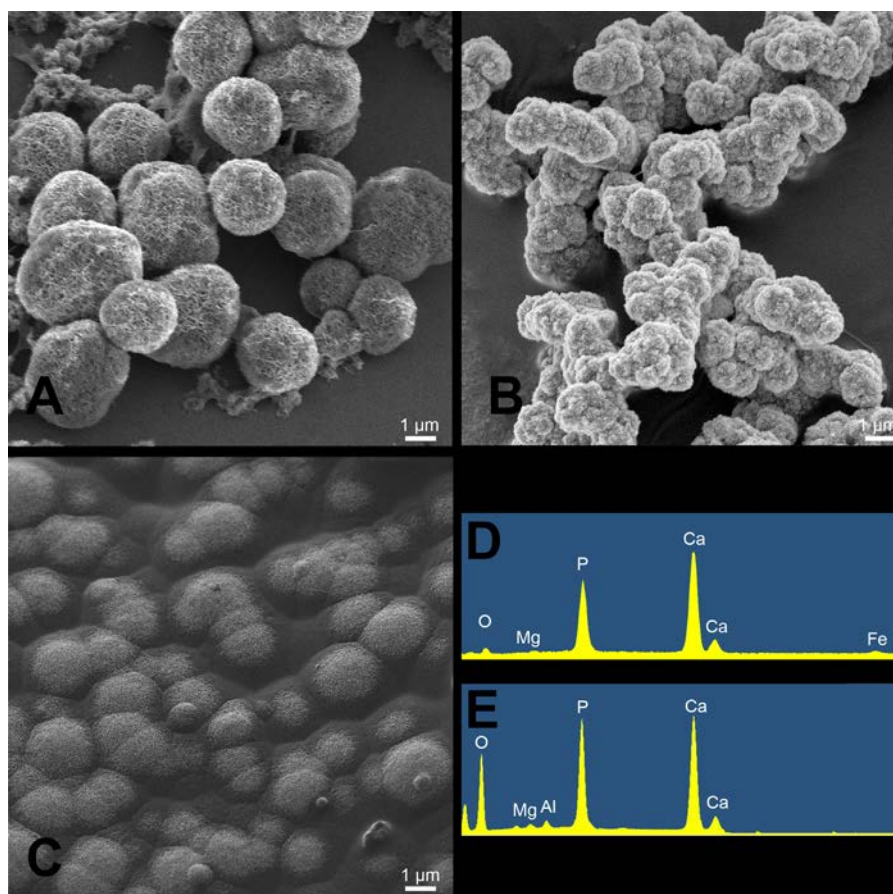


**Figure 3** Scanning electron microscopy of calcospherites developed on a polymer. A) Control calcospherites composed of HA tablets developed in a standard body fluid. B) Calcospherites developed in the presence of iron in the body fluid; note the reduced size indicating an interaction with mineralization. C) Surface of the polymer incubated in the presence of  $\text{Al}^{3+}$ ; there is an almost complete inhibition of the calcospherites growth. D) EDS analysis of the calcospherites in B indicating the presence of traces of iron in HA composed of calcium/phosphate stabilized with magnesium. E) EDS analysis of the mineral developed in C indicating the presence of trace of aluminum together with calcium, phosphate and magnesium.

*Microscopie électronique à balayage de calcosphérites développés sur un polymère fonctionnalisé avec des groupements  $-\text{COOH}$ . A) Les calcosphérites sont présents à la surface du matériau et se développent par nucléation successive dans le liquide biologique. B) Croissance des calcosphérites en présence de fer à l'intérieur du milieu de culture. La présence du fer réduit considérablement leur taille. C) Absence de développement de calcosphérites lorsque des ions aluminium sont ajoutés dans le milieu de culture. La surface du polymère, avec quelques traces calcifiées, est bien visible. D) Analyse EDS des calcosphérites présents sur la Fig. B : notez la présence d'un petit pic de fer dans l'hydroxyapatite composée de calcium et phosphate stabilisé par du magnésium. E) Analyse EDS des calcosphérites présents sur la Fig. C : la présence d'aluminium est aussi mise en évidence lorsque la concentration est supérieure à 0,05 % des atomes.*

methacrylate–pHEMA) which can be chemically modified by carboxymethylation. Carboxymethylated pHEMA reproduces the structure of acid proteins of the bone matrix known to induce mineralization (e.g. BSP) [20]. When placed in a synthetic body fluid having the same ionic composition than the extracellular fluids, pellets made of this polymer induce mineralization. Calcified globules made of HA develop on the polymer surface within 15 days (Fig. 3A). These mineralized globules are similar in size and composition to the calcospherites described in the cartilaginous growth plate of long bones. Calcospherites are also observed in the woven bone of rapidly forming bones (callus, metaplasia...). The carboxymethylated pHEMA model has been used to evaluate the effects of drugs known to interfere with

calcification [21] and also metal ions which can be dissolved in the body fluid.  $\text{Fe}^{3+}$  ions at the concentration of 20, 40 or  $60 \mu\text{M/L}$  reduce the size of the calcospherites (Fig. 3B) [22]. SEM-EDS identified iron in the calcospherites at very low amount ( $> 0.05$  atomic %) (Fig. 3D). Cobalt, nickel and chromium (these metals present in stainless-steel orthopedic prostheses) can also modify the size of calcospherites [23]. Strontium has also an effect on the calcospherites in a dose dependent manner. However,  $\text{Sr}^{2+}$  can be progressively eluted from the crystals [24].

We have recently investigated the influence of aluminum in this model [25]. Aluminum chloride was added in the body fluid at the concentration of 20, 40, and  $60 \mu\text{g/L}$   $\text{Al}^{3+}$ . Aluminum strongly reduced the growth of calcospherites



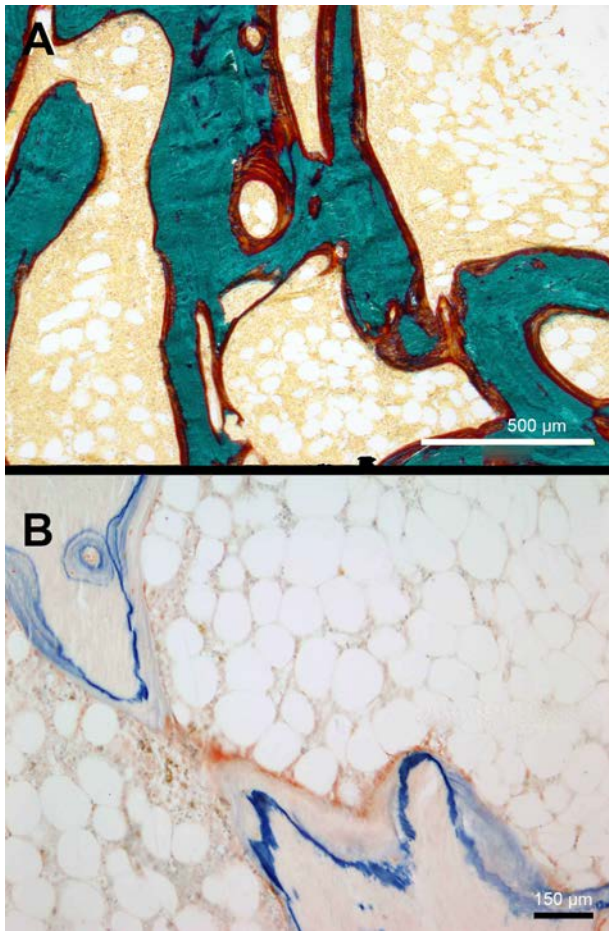


**Figure 4** A) Osteomalacia in a patient with dialyzed renal insufficiency. Goldner's trichrome identifies mineralized bone matrix in green and osteoid tissue in red; undecalcified section. Note the considerable amount of osteoid tissue and the thickness of osteoid seams indicating a mineralization defect. B) Histochemical identification of aluminum by the solochrome azurine method.  $\text{Al}^{3+}$  is in blue, bone is faintly stained in orange. A) *Ostéomalacie chez un patient dialysé pour une insuffisance rénale chronique. Trichrome de Goldner : la matrice osseuse minéralisée est en vert, le tissu ostéoïde en rouge sur des coupes non décalcifiées. B) Identification histochimique de l'aluminium par la coloration au solochrome azurine.  $\text{Al}^{3+}$  apparaît sous forme de bandes bleues, l'os est très légèrement coloré en orange. Notez la quantité considérable de tissu ostéoïde et l'épaisseur des bordures ostéoïdes indiquant un trouble de minéralisation.*

(and the highest concentration has completely inhibited their formation) (Fig. 3D). SEM-EDS identified  $\text{Al}^{3+}$  in the HA calcospherites (Fig. 3E). Furthermore, other pellets were incubated with pieces of aluminum foil and, here again, a strong inhibition of the calcospherite formation was observed. This indicates that  $\text{Al}^{3+}$  can be released from aluminum foils by oxidation in the body fluid.

## Bone, aluminum and kidney

During the 1970s, a series of patients with renal insufficiency, who were dialyzed, developed the dialysis

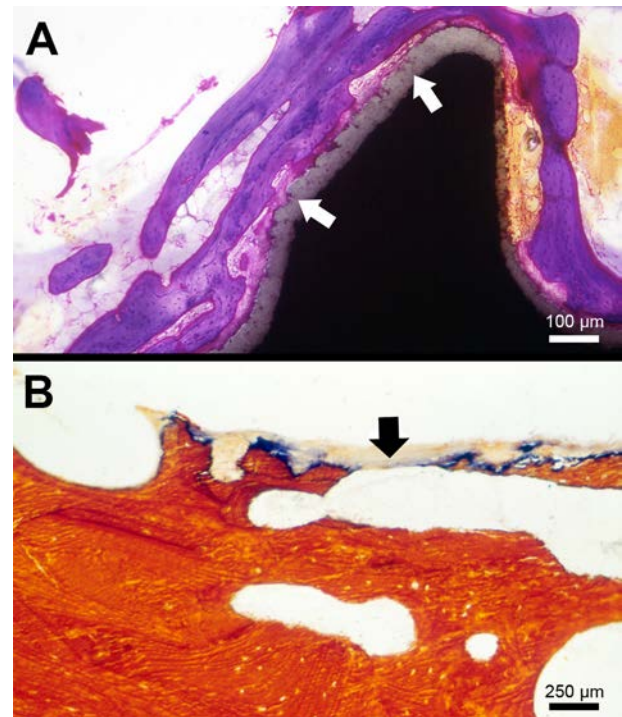


**Figure 5** A) A threaded hip prosthesis covered by a thick coating of alumina deposited by a plasma torch (arrows). Thick and polished section after undecalcified embedding; the metal is in black. B) Histochemical identification of aluminum by the solochrome azurine method in another patient who had the same type of prosthesis. The metallic part has been removed before embedding and sectioning at a  $7\text{ }\mu\text{m}$  thickness.  $\text{Al}^{3+}$  is in blue, the calcified bone matrix in orange and non-mineralized bone is unstained (arrow) and forms a thick layer facing the prosthesis, indicating a localized mineralization defect.

A) *Prothèse de hanche filetée recouverte par un épais dépôt d'alumine déposé par torche à plasma (flèches) ; tranche épaisse et polie sans décalcification. Le métal apparaît en noir. B) Identification histochimique de l'aluminium par la technique au solochrome azurine. La partie métallique a été enlevée avant inclusion pour réaliser des coupes de  $7\text{ }\mu\text{m}$  d'épaisseur.  $\text{Al}^{3+}$  est en bleu, la matrice calcifiée en orange et l'os non minéralisé est incolore (flèche) indiquant un défaut local de minéralisation.*

encephalopathy associated with osteomalacia (a mineralization defect characterized by an accumulation of osteoid tissue) (Fig. 4A) [26,27]. Encephalopathy was related to the aluminum content in the dialysate because water, at the time, was purified by alumina gels in the water treatment plants. Dialysis patients had an additional cause of aluminum intoxication: they were treated by aluminum hydroxide as a countermeasure for hyperphosphatemia. In the bone from patients with dialysis osteomalacia, the presence of aluminum was identified as linear bands by histochemical methods; this reflects the deposition of  $\text{Al}^{3+}$  along the calcification front and cement lines within the calcified bone matrix (Fig. 4B) [9,11]. In dialyzed patients, iron and fluoride were also identified by several authors but the consensus was that aluminum had the most deleterious effects on bone mineralization [28]. Aluminum was also found to interfere

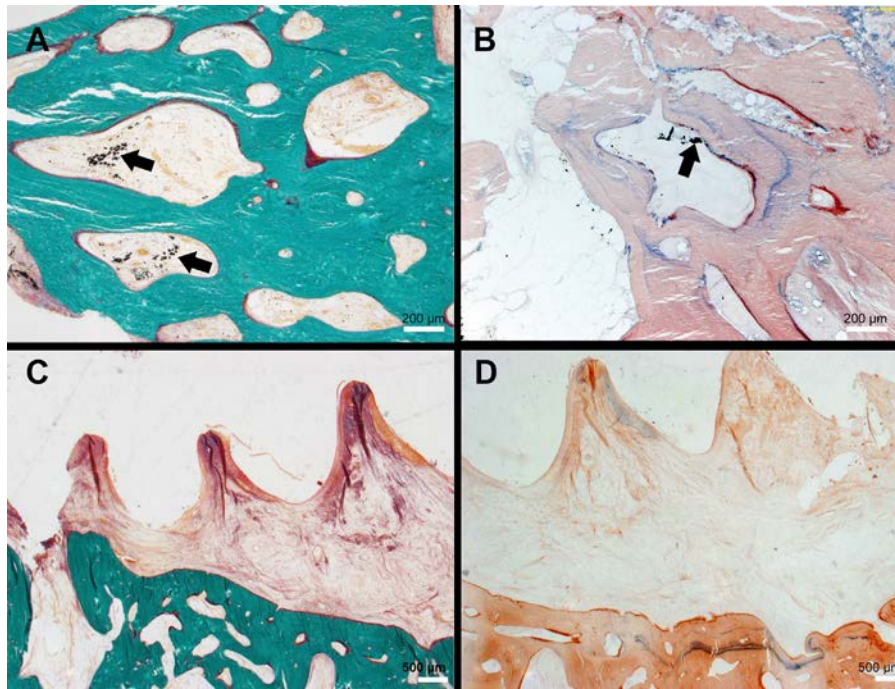


**Figure 6** A) Bone harvested in the vicinity of a TA6V hip prosthesis replaced during a hip prosthesis revision. Arrows identify black metallic debris in the marrow contained in the Haversian canals. Goldner's trichrome, undecalcified bone. B) Section from the same patient, metallic wear debris composed of TA6V are evidenced (arrow). Blue bands of aluminum are present in the calcified bone matrix of the Haversian canal surrounding the metal particles. Solochrome azurine staining. C) Bone harvested from the femoral head of a patient treated by a threaded screw for a hip fracture several years ago. Fibrosis has developed inside the threads (the metal has been removed). Goldner's trichrome, undecalcified section. D) Section from the same patient stained with solochrome azurine. Aluminum deposits are visible as blue bands in the bone facing the screw. The soft tissues (which do not contain calcium phosphate) are unstained.

*A) Tissu osseux prélevé au voisinage d'une prothèse en TA6V utilisée pour le traitement d'une fracture de hanche. La vis a été laissée en place pendant de nombreuses années. Les flèches identifient des débris métalliques dans les canaux de Havers. Trichrome de Goldner, coupe non décalcifiée. B) Coupe voisine obtenue chez le même patient ; les débris métalliques sont constitués de particules d'usure du TA6V (flèche). Des bandes bleues (aluminium) sont présentes dans la matrice osseuse calcifiée, des canaux de Havers autour des particules métalliques ; coloration au solochrome azurine. C) Fragment de tête fémorale d'un patient traité par une vis filetée pour une fracture du col fémoral survenue de nombreuses années auparavant. Une fibrose s'est développée à l'intérieur du filetage (le métal a été enlevé avant l'inclusion). Coloration de Goldner, coupe non décalcifiée. D) Coupe adjacente provenant du même patient et colorée par le solochrome azurine. Des dépôts d'aluminium sont visibles sous forme de bandes bleues dans le tissu osseux en face de la vis. Les tissus mous (ne contenant pas de phosphate de calcium) sont incolores.*

directly with bone remodeling by reducing bone formation by osteoblasts [29,30]. An indirect effect was also identified as aluminum can accumulate in the parathyroid glands and alters the parathyroid hormone levels by reducing its synthesis [31].

## Bone, aluminum and biomaterials

Several reports have stressed the importance of aluminum released by biomaterials as a toxic for bone. A ceramic coating of prosthetic stems has been proposed to favor osseointegration. HA and alumina coatings were widely used in the 1990s. However, alumina-coated prostheses were associated with a juxta prosthetic mineralization defect (similar to the dialysis osteomalacia) due to an accumulation of  $Al^{3+}$  in the anchoring bone. A direct release of  $Al^{3+}$  from the coating was found after histochemical staining (Fig. 5) [32,33]. A bone cement containing aluminum fluorosilicate

was used in oto-surgery and caused several lethal cases of aluminum encephalopathy [34].

Biomaterials are now widely used in biomedicine and their applications are numerous: heart valves, artificial heart, dental and orthopedic implants, tracheal and vascular prostheses. ... More than half of biomaterials produced by industry are used in an intra-osseous site (cement, synthetic bone filling material or prosthesis). Biomaterials are inert objects placed in direct contact with the biological fluids. They can attack the surface of metallic biomaterials as they contain numerous anions ( $Cl^-$ ,  $PO_4^{3-}$ ,  $HCO_3^-$ ,  $SO_4^{2-}$ ...), cations ( $Mg^{2+}$ ,  $Na^+$ ,  $Ca^{2+}$ ,  $Fe^{3+}$ ...), dissolved oxygen and free radical oxygen species. This liquid microenvironment appears to have an oxidizing power equal to 1/3 this of the ocean water and 1/4 this of the air [35]. In addition, the body temperature increases the oxidizing capacity and local pH variations are frequent [36]. Corrosion of metallic biomaterials can occur in different types of conditions: at the metal joint grains (as metals are polycrystalline), by



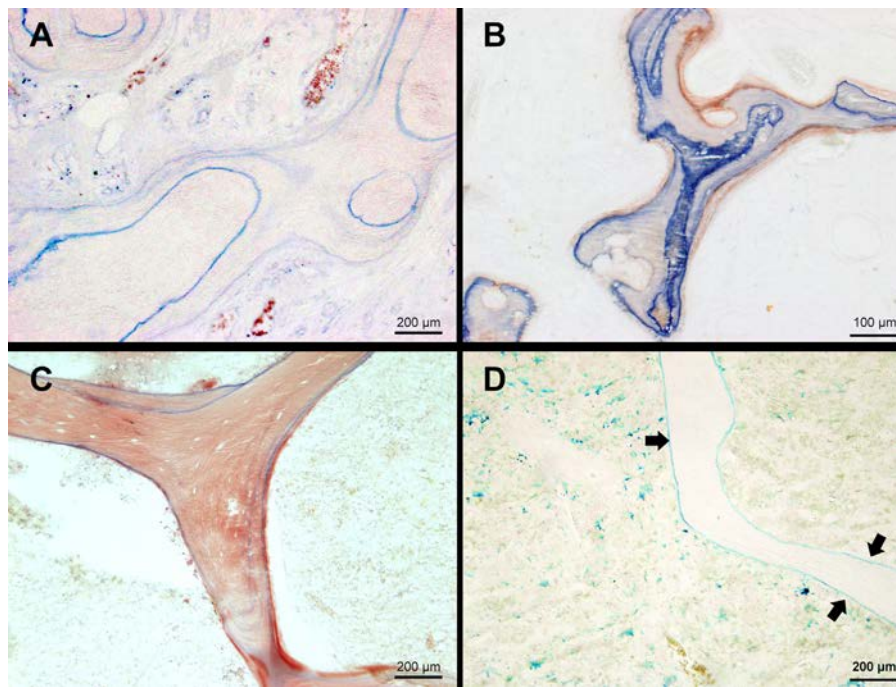


**Figure 7** A) Genetic hemochromatosis with osteoporosis. Perl's staining identifies numerous bands of iron deposited in the bone matrix. B) Histochemical detection of aluminum by solochrome azurine in the same patient. C) Histochemical detection of aluminum in a case of sickle cell anemia. D) Histochemical detection of iron (Perl's staining) in the same patient. Note the blue lines (arrows) indicating the presence of iron in the bone matrix (unstained) and the presence of numerous siderophages containing iron in the bone marrow (blue spots).

*A) Hémochromatose génétique avec ostéoporose. Coloration de Perl's identifiant de nombreuses bandes de fer dans la matrice osseuse. B) Détection histochimique de l'aluminium par le solochrome azurine chez le même patient. C) Détection histochimique de l'aluminium dans un cas de drépanocytose. D) Détection histochimique du fer (coloration de Perl's) chez le même patient. Notez la présence de lignes bleues (flèches) indiquant la présence de fer dans la matrice osseuse non colorée et la présence de nombreux sidérophages intramédullaires contenant du fer (tâches bleues).*

galvanic currents (if different metals are present, by a local electrolytic phenomenon) and by the generation of wear debris from articulating biomaterials (especially in the case of orthopedic prosthesis).

We have recently reported a series of 32 patients with a revision for a total reconstruction after aseptic loosening of an alumina-on-alumina hip prosthesis [37]. This type of prosthesis is known to have the best friction torque [38,39]. In these patients, the periprosthetic tissues were analyzed in the search of alumina debris. In 14 patients, a small fragment of periprosthetic bone was also analyzed after undecalcified embedding. Sections were obtained on a heavy duty microtome and stained by a Goldner's trichrome (for the identification of osteoid tissue and mineralized phase), solochrome azurine staining (for identification of  $Al^{3+}$ ) and Perls' staining. Alumina grains were never encountered in the soft tissues. Metal particles were present in 3 patients and SEM-EDS revealed that they were composed of the TA6V titanium alloy containing 6% aluminum and 4% vanadium. TA6V (or grade V titanium ASTM) is the metal used in orthopedics for prostheses, screws, cups...). Histochemical analysis revealed that the  $Fe^{3+}$  was not present in the bone matrix but aluminum bands were observed for each patient. In a control series of 8 patients having received a prosthesis without alumina (e.g., metal-on-polyethylene or metal-on-metal), the same methodology of analysis was

used.  $Al^{3+}$  was also identified in the bone matrix from these patients as linear bands in the vicinity of the prosthesis or the metal wear debris (Fig. 6A–B). It is likely that  $Al^{3+}$  comes from oxidation of the metallic parts of the prosthesis (stem, cup, screw) and an origin from the alumina cannot be excluded. However, the long term tolerance of the alumina-on-alumina prostheses, and the fact that the amount of aluminum bands in the bone matrix were similar in the other group, is a plea for an oxidation of the TA6V rather than a ionic decomposition of this very stable alumina [40]. The  $Al^{3+}$  ion release from alumina-on-alumina and metal-on-metal total hip prostheses was dosed in the serum from a series of patients and the  $Al^{3+}$  content was not different between the two groups and with a control group without prosthesis [41].

Presence of aluminum in the bone matrix is also common in orthopedic samples obtained after ablation of titanium material. Fig. 6C–D illustrates the release of aluminum from a threaded screw in a femoral head placed more than ten years before for treating a hip fracture. The material was changed during revision for a total hip arthroplasty. In such cases, the continuous release of aluminum from the metallic biomaterial is proven by the deposition of numerous repetitive bands mimicking the growth lines on a tree trunk. In a compilation study, the release of metal ions was confirmed in the body fluids of patients with metallic biomaterials



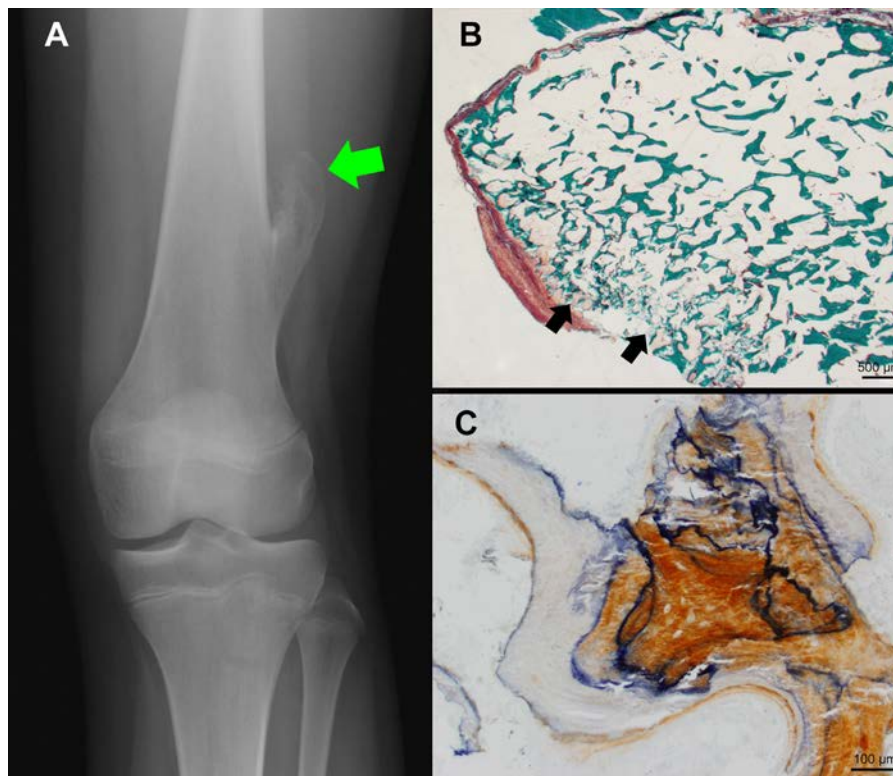


**Figure 8** A) X-ray image of an isolated exostosis of the lower femoral extremity in a 13 years-old-child. B) A whole exostosis studied undecalcified. The dystrophic proliferative cartilage is indicated by arrows. A thin shell of cortical bone surrounds a trabecular network. Goldner's staining. C) Histochemical identification of aluminum by the solochrome azurine method in this exostosis.

*A) Radiographie d'une exostose isolée de l'extrémité fémorale inférieure chez un enfant de 13 ans (flèche verte). B) Exostose complète étudiée sans décalcification. La couche de cartilage dystrophique proliférative est indiquée par des flèches. Une fine coque de tissu osseux cortical entoure un réseau trabéculaire. Trichrome de Goldner. C) Identification histochimique de l'aluminium par le solochrome azurine dans l'os trabéculaire de l'exostose.*

by various techniques including Inductively Coupled Plasma Mass Spectrometry (ICP-MS) and graphite furnace atomic absorption spectrometry (GF-AAS) [42]. Although titanium is protected by a film of titanium oxides, the TA6V-based devices can release aluminum after prolonged implantation [43].

This will certainly be observed in the next future in dental implantology. Classically, dental implants were prepared with c.p. grade II titanium. It is more ductile than the TA6V alloy (grade V), which contains aluminum and vanadium. Some industrial companies have recently proposed TA6V implants on the market, especially short implants to be used in areas with a low bone mass. Titanium can be easily oxidized and altered in mouth by the action of numerous oxidants (fluoride containing toothpastes, reactive oxygen species from polymorphonucleated cells and bacteria, or organic acids of the saliva) [44]. The release of aluminum from TA6V dental implants could represent a sanitary problem in the next decade.

### Bone, aluminum and diseases associated with iron metabolism

Genetic hemochromatosis (GH) is an autosomal recessive disease responsible for an iron overload. The most frequent

form is due to a mutation of the *HFE* gene. In these patients, osteopenia and osteoporosis are frequent (28–50% of patients), together with the liver disease which is the more severe factor [45]. A positive iron staining is reported in the bone matrix of these patients and appears to form linear bands. Surprisingly, aluminum can also be detected as linear bands in the same areas in some patients (Fig. 7).

$\text{Fe}^{3+}$  is also identified by histochemistry in the bone matrix of patients with other iron-related diseases such as  $\beta$ -thalassemia and sickle cell anemia [46,47]. The mechanisms of the  $\text{Fe}^{3+}$  localization in bone are not clearly understood but the role of metal transporter proteins (such as ferroportin) has been recently reviewed [48]. In two patients with sickle cell anemia, a colocalization of  $\text{Al}^{3+}$  with  $\text{Fe}^{3+}$  in bone was observed in our laboratory.

### Bone, aluminum and digestive diseases

Aluminum is absorbed by the gut as evidenced by a number of papers in the rat [49,50]. It is also absorbed in humans as shown in patients receiving phosphate binders in dialysis patients [51]. Aluminum absorption from the gut leads to a bone deposition, even in the presence of a normal kidney function.  $\text{Al}^{3+}$  absorption was increased in a patient with a peptic ulcer and a long-term history of gastroprotection

[52]. We reported a patient with a celiac disease who was using oral medications containing aluminum. She developed osteoporosis with very low bone mineral density values (T score = -6.18 at the lumbar spine).  $Al^{3+}$  was identified by solochrome azurine staining in a transiliac bone biopsy [53]. We also observed similar findings in a patient with low bone mineral density (T score = -3.56 at the lumbar spine) and fractures of the *os ilium*. The patient had also a long history of dyspepsia and was using aluminum-containing gastroprotectors for decades; here again,  $Al^{3+}$  was identified in the bone biopsy. Parenteral nutrition is also associated with an increased aluminum absorption (released from nutrition solutions containing contaminated casein, from glass vials...) [54]. Aluminum has also been identified as a possible environmental causal factor in Crohn's disease [55]. Aluminum enhances colic inflammation in mice [56]. Lessons from the past (dialysis patients) and from animal studies indicate that chronic accumulation of aluminum in the bone is likely to occur in patients with inflammatory diseases of the digestive tract. Although these inflammatory bowel diseases are known to induce osteoporosis by themselves [57], it is most probable that aluminum deposition in the bone matrix contributes to the bone loss. However, this remains to be proven by bone biopsy studies.

## Calcified bone in exostosis

Exostosis is the most frequent benign tumor in children and adults. Isolated exostosis is frequent but multiple exostoses are observed in several types of Multiple Hereditary Exostosis (MHE). MHE is an autosomal genetic disease due to mutation in the Golgi-associated heparin sulfate polymerases (EXT1, EXT2 or EXT3) [58]. Although the pathogenesis of isolated and MHE are not fully understood, these tumors share common characteristics: they are covered by a cape of proliferation cartilage, they possess a shell of cortical bone which surround a more or less developed network of trabecular bone containing bone marrow. We have recently reported a series of thirty patients with either isolated or multiple exostosis (three cases of MHE) [19]. Histological analysis of the undecalcified tumor revealed the presence of aluminum in the bone matrix of the tumor in 2/3 of patients. Surprisingly, iron was also deposited in the same areas in 1/3 of the patients (Fig. 8). Because a dysregulation of the osteo-progenitor cell has been described in this disease, it is most probable that metabolic changes in the osteoblast function are responsible for the abnormal deposition of these two metals.

## The origin of aluminum in bone

It is now well recognized that aluminum enters in the body from different sources. As mentioned above, aluminum is present in foods and beverages (the additive E173 is aluminum oxide) but other routes of penetration in the body have been identified: trans or percutaneous absorption (from vaccines and anti-sweating or antiperspirant products, e.g. alum stone) and locally released from metallic biomaterials. In the body, 95% of ingested aluminum is eliminated in the feces and the 5% remaining circulate in the blood mainly bound to transferrin and albumin (Fig. 9

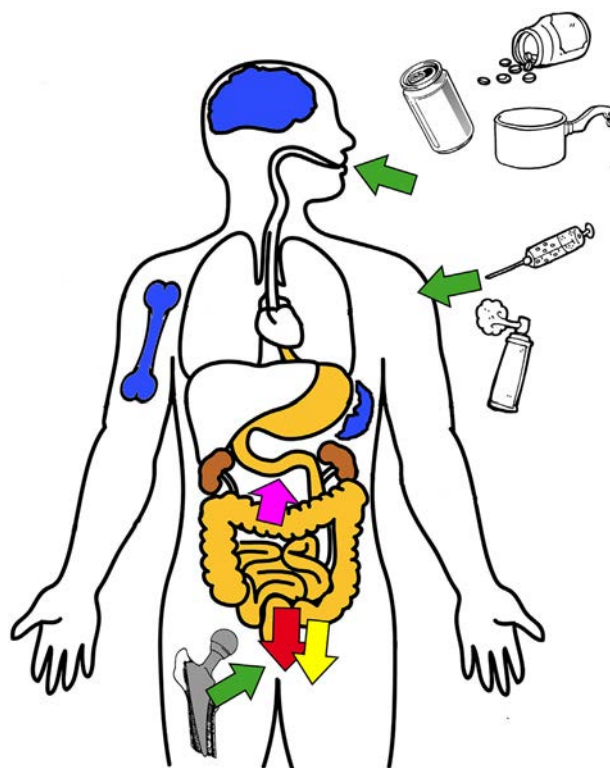


**Figure 9** Metabolism of aluminum in humans. Green arrows: input sources are either by ingestats (water, food, drugs...), of cutaneous origin (vaccines, deodorant, antiperspirant...) or internal release from TA6V titanium devices. Red arrow: 95% of the ingested aluminum is excreted in the feces. Pink arrow: 4% of the absorbed aluminum circulates in the blood bound to transferrin (80%), albumin (10%) and other proteins (10%). Yellow arrow: 83% of the circulating aluminum is excreted in urine. Blue organs: aluminum can be deposited in three main tissues: central nervous system, spleen and bone.

*Métabolisme de l'aluminium chez l'homme. Les flèches vertes indiquent les sources d'entrée de l'aluminium dans l'organisme soit à partir des ingestats (eau, nourriture, médicament...), voie cutanée (vaccin, déodorant ou antiperspirant...) ou endogènes par relargage de l'aluminium à partir de biomatériaux en titane. Flèche rose : 5 % de l'aluminium absorbé circule dans le sang, lié à la transferrine (80 %), à l'albumine (10 %) et à d'autres protéines (10 %). Flèche rouge : 95 % de l'aluminium ingéré est excrété dans les fèces. Flèche jaune : 83 % de l'aluminium circulant est excrété dans les urines. Les organes en bleus représentent les cibles dans lesquelles l'aluminium non éliminé peut se déposer : système nerveux central, rate et matrice osseuse.*

summarizes the aluminum metabolism in the body). The circulating aluminum can mainly be fixed in two preferential organs: brain and bone. The metal is recognized as a neurotoxic in Alzheimer and Parkinson diseases where it can also colocalize with iron. In bone, aluminum is a cause of bone loss in laboratory animals and humans and high doses cause osteomalacia. Finally, there are a number of strange coincidences concerning the metabolism of these two metals in the body: same transporters, cytotoxic activity,

impairment of osteoblastic activity at low dose, inhibition of bone mineralization at high doses.

## Conclusion

Aluminum can bind to the phosphate groups of HA of the calcified bone matrix. Histochemical methods are by far superior to spectroscopic methods (EDS and WDS) because aluminum and iron are identified in the same location of the bone matrix. Although the pathophysiological mechanisms are not fully understood at the cellular and molecular levels, colocalization of aluminum and iron is certainly not the fruit of chance and much effort is still needed to improve our knowledge on the toxic activity of metals.

## Disclosure of interest

The authors declare that they have no competing interest.

## Acknowledgments

This review was presented as an oral communication at the Keele Meeting in Lille (February–March 2015). Many thanks to Mrs. Lechat for secretarial assistance. We also thank all surgeons or clinicians who addressed bone samples to our laboratory and especially D. Moukoko, N. Henric, V. Steiger, P. Le Nay, J.M. Frin, C. De Bodman, D. Mulleman, M. Audran, E. Legrand, B. Bouvard. This research was funded by the Ministère de l'Enseignement Supérieur et de la Recherche.

## References

- [1] Gordon JA, Tye CE, Sampaio AV, Underhill TM, Hunter GK, Goldberg HA. Bone sialoprotein expression enhances osteoblast differentiation and matrix mineralization in vitro. *Bone* 2007;41:462–73.
- [2] Whyte MP. Physiological role of alkaline phosphatase explored in hypophosphatasia. *Ann N Y Acad Sci* 2010;1192:190–200.
- [3] Elliott JC. Structure and chemistry of the apatites and other calcium orthophosphates. *Studies in Inorganic Chemistry*, Vol. 18. Amsterdam, London, NY, Tokyo: Elsevier; 2013.
- [4] Age P. Histochemistry: theoretical and applied. Edinburgh: Churchill Livingstone; 1968.
- [5] de Vernejoul MC, Pointillart A, Golenzer CC, Morieux C, Bielakoff J, Modrowski D, et al. Effects of iron overload on bone remodeling in pigs. *Am J Pathol* 1984;116:377–84.
- [6] Guggenbuhl P, Fergelot P, Doyard M, Libouban H, Roth MP, Gallois Y, et al. Bone status in a mouse model of genetic hemochromatosis. *Osteoporos Int* 2010;22:2313–9.
- [7] Horobin RW. Understanding histochemistry. In: Selection, evaluation and design of biological stains. Chichester, NY: Hortwood; 1988.
- [8] Pemmer B, Roschger A, Wastl A, Hofstaetter J, Wobraschek P, Simon R, et al. Spatial distribution of the trace elements zinc, strontium and lead in human bone tissue. *Bone* 2013;57:184–93.
- [9] Malluche HH. Aluminium and bone disease in chronic renal failure. *Nephrol Dial Transplant* 2002;17:21–4.
- [10] Lillie R, Mowry R. Histochemical studies on absorption of iron by tissue sections. *Bull Int AM Mus* 1949;30:91.
- [11] Faugère MC, Malluche HH. Stainable aluminum and not aluminum content reflects bone histology in dialyzed patients. *Kidney Int* 1986;30:717–22.
- [12] Horobin RW, Kiernan JA, Chrome Azurol B. Conn's biological stains: a handbook of dyes, stains and fluorochromes for use in biology and medicine. 10th Ed. Biological Stain Commission; 2002. p. 208–9.
- [13] Denton J, Freemont AJ, Ball J. Detection and distribution of aluminium in bone. *J Clin Pathol* 1984;37:136–42.
- [14] Ellis H, Pang M, Mawhinney W, Skillen A. Demonstration of aluminium in iliac bone: correlation between aluminon and solochrome azurine staining techniques with data on flameless absorption spectrophotometry. *J Clin Pathol* 1988;41:1171–5.
- [15] Fernandez-Martin J, Menendez P, Acuna G, Canteros A, Gómez C, Cannata J. Staining of bone aluminium: comparison between aluminon and solochrome azurine and their correlation with bone aluminium content. *Nephrol Dial Transplant* 1996;11:80–5.
- [16] Romanski SA, McCarthy JT, Kluge K, Fitzpatrick LA. Detection of subtle aluminum-related renal osteodystrophy. *Mayo Clin Proc*, Vol. 68. Elsevier; 1993. p. 419–26.
- [17] Heinrich KF. Electron beam X-ray microanalysis. Atlanta, GA: Van Nostrand Reinhold Co., Atlanta Book Company; 1981.
- [18] Goldstein J, Newbury D, Echlin P, Joy D, Fiori C, Lifshin E. Scanning electron microscopy and X-ray microanalysis. A text for biologists, materials scientists, and geologists. NY: Plenum Press; 1981.
- [19] Chappard D, Mabilieu G, Moukoko D, Henric N, Steiger N, Le Nay P, et al. Aluminum and iron can be deposited in the calcified matrix of bone exostoses. *J Inorg Biochem* 2015;152:174–9.
- [20] Filmon R, Grizon F, Baslé MF, Chappard D. Effects of negatively charged groups (carboxymethyl) on the calcification of poly(2-hydroxyethyl methacrylate). *Biomaterials* 2002;23:3053–9.
- [21] Filmon R, Baslé MF, Barbier A, Chappard D. In vitro study of the effect of bisphosphonates on mineralization induced by a composite material: poly 2(hydroxyethyl) methacrylate coupled with alkaline phosphatase. *Morphologie* 2000;84:23–33.
- [22] Guggenbuhl P, Filmon R, Mabilieu G, Baslé MF, Chappard D. Iron inhibits hydroxyapatite crystal growth in vitro. *Metabolism Clin Exp* 2008;57:903–10.
- [23] Mabilieu G, Filmon R, Petrov PK, Baslé MF, Sabokbar A, Chappard D. Cobalt, chromium and nickel affect hydroxyapatite crystal growth in vitro. *Acta Biomater* 2010;6:1555–60.
- [24] Beuvelot J, Filmon R, Mauras Y, Baslé MF, Chappard D. Adsorption and release of strontium from hydroxyapatite crystals developed in Simulated Body Fluid (SBF) on poly (2-hydroxyethyl) methacrylate substrates. *Dig J Nanomater Biostruct* 2013;8:207–17.
- [25] Degeratu CN, Mabilieu G, Cincu C, Chappard D. Aluminum inhibits the growth of hydroxyapatite crystals developed on a biomimetic methacrylic polymer. *J Trace Elem Med Biol* 2013;27:346–51.
- [26] Alfrey AC, LeGendre GR, Kaehny WD. The dialysis encephalopathy syndrome. Possible aluminum intoxication. *N Engl J Med* 1976;294:184–8.
- [27] Ward M, Ellis H, Feest T, Parkinson I, Kerr D, Herrington J, et al. Osteomalacic dialysis osteodystrophy: evidence for a water-borne aetiological agent, probably aluminium. *Lancet* 1978;311:841–5.
- [28] Cannata Andia JB. Aluminium toxicity: its relationship with bone and iron metabolism. *Nephrol Dial Transplant* 1996;11(Suppl. 3):69–73.
- [29] Li X, Han Y, Guan Y, Zhang L, Bai C, Li Y. Aluminum induces osteoblast apoptosis through the oxidative stress-mediated JNK signaling pathway. *Biol Trace Elem Res* 2012;150:502–8.
- [30] Rodriguez M, Felsenfeld AJ, Llach F. Aluminum administration in the rat separately affects the osteoblast and bone mineralization. *J Bone Miner Res* 1990;5:59–67.
- [31] Diaz-Corte C, Fernandez-Martin J, Barreto S, Gomez C, Fernandez-Coto T, Braga S, et al. Effect of aluminium load

- on parathyroid hormone synthesis. *Nephrol Dial Transplant* 2001;16:742–5.
- [32] Frayssinet P, Tourenne F, Rouquet N, Bonel G, Conte P. Biological effects of aluminium diffusion from plasma-sprayed alumina coatings. *J Mater Sci Mater Med* 1994;5:491–4.
- [33] Savarino L, Cenni E, Stea S, Donati ME, Paganetto G, Moroni A, et al. X-ray diffraction of newly formed bone close to alumina- or hydroxyapatite-coated femoral stem. *Biomaterials* 1993;14:900–5.
- [34] Hantson P, Mahieu P, Gersdorff M, Sindic C, Lauwerys R. Fatal encephalopathy after otoneurosurgery procedure with an aluminum-containing biomaterial. *Clin Toxicol* 1995;33:645–8.
- [35] Hanawa T, Kaga M, Itoh Y, Echizenya T, Oguchi H, Ota M. Cytotoxicities of oxides, phosphates and sulphides of metals. *Biomaterials* 1992;13:20–4.
- [36] Tengvall P, Lundstrom I, Sjoqvist L, Elwing H, Bjursten LM. Titanium-hydrogen peroxide interaction: model studies of the influence of the inflammatory response on titanium implants. *Biomaterials* 1989;10:166–75.
- [37] Bizot P, Chappard D. In vivo local release of aluminum ions from alumina-on-alumina hip replacement. *European Orthopaedic Research Society (EORS)*; 2014.
- [38] Bizot P, Banallec L, Sedel L, Nizard R. Alumina-on-alumina total hip prostheses in patients 40 years of age or younger. *Clin Orthop Relat Res* 2000;68–76.
- [39] Sedel L. Evolution of alumina-on-alumina implants: a review. *Clin Orthop Relat Res* 2000;48–54.
- [40] Boutin P. Total arthroplasty of the hip by fritted alumina prosthesis. Experimental study and 1st clinical applications. *Orthop Traumatol Surg Res* 1972;58:229–46.
- [41] Savarino L, Greco M, Cenni E, Cvasinni L, Rotini R, Baldini N, et al. Differences in ion release after ceramic-on-ceramic and metal-on-metal total hip replacement. Medium-term follow-up. *J Bone Joint Surg Br* 2006;88:472–6.
- [42] Matusiewicz H. Potential release of in vivo trace metals from metallic medical implants in the human body: From ions to nanoparticles—A systematic analytical review. *Acta Biomater* 2014;10:2379–403.
- [43] Okazaki Y, Gotoh E. Comparison of metal release from various metallic biomaterials in vitro. *Biomaterials* 2005;26:11–21.
- [44] Mabilieu G, Bourdon S, Joly-Guillou ML, Filmon R, Baslé MF, Chappard D. Influence of fluoride, hydrogen peroxide and lactic acid on the corrosion resistance of commercially pure titanium. *Acta Biomater* 2006;2:121–9.
- [45] Guggenbuhl P, Brissot P, Loreal O. Miscellaneous non-inflammatory musculoskeletal conditions. *Haemochromatosis* the bone and the joint. *Best Pract Res Clin Rheumatol* 2011;25:649–64.
- [46] Mahachoklertwattana P, Sirikulchayanonta V, Chuansumrit A, Karnsombat P, Choubtum L, Sriphrapadang A, et al. Bone histomorphometry in children and adolescents with beta-thalassemia disease: iron-associated focal osteomalacia. *J Clin Endocrinol Metab* 2003;88:3966–72.
- [47] Rioja L, Girot R, Garabédian M, Cournot-Witmer G. Bone disease in children with homozygous  $\beta$ -thalassemia. *Bone Miner* 1990;8:69–86.
- [48] Loréal O, Cavey T, Bardou-Jacquet E, Guggenbuhl P, Ropert M, Brissot P. Iron, hepcidin, and the metal connection. *Front Pharmacol* 2014;5:128.
- [49] Arnich N, Cunat L, Lanhers MC, Burnel D. Comparative in situ study of the intestinal absorption of aluminum, manganese, nickel, and lead in rats. *Biol Trace Elem Res* 2004;99:157–71.
- [50] Provan SD, Yokel RA. Aluminum uptake by the in situ rat gut preparation. *J Pharmacol Exp Ther* 1988;245:928–31.
- [51] Drueke TB. Intestinal absorption of aluminium in renal failure. *Nephrol Dial Transplant* 2002;17:13–6.
- [52] Recker RR, Blotcky AJ, Leffler JA, Rack EP. Evidence of aluminum absorption from the gastrointestinal tract and bone deposition by aluminum carbonate ingestion with normal renal function. *J Lab Clin Med* 1977;90:810–5.
- [53] Chappard D, Insalaco P, Audran M. Aluminum osteodystrophy and celiac disease. *Calcif Tissue Int* 2004;74:122–3.
- [54] Kruger PC, Parsons PJ, Galusha AL, Morrisette M, Recker RR, Howard LJ. Excessive aluminum accumulation in the bones of patients on long-term parenteral nutrition: postmortem analysis by electrothermal atomic absorption spectrometry. *J Parenter Enteral Nutr* 2013;38:728–35.
- [55] Lerner A. Aluminum is a potential environmental factor for Crohn's disease induction - extended hypothesis. In: Shoenfeld Y, Gershwin ME, editors. *Autoimmunity, Pt C: The mosaic of Autoimmunity*, Vol. 1107. 2007. p. 329–45.
- [56] Pineton de Chambrun G, Body-Malapel M, Frey-Wagner I, Djouina M, Deknuydt F, Atrott K, et al. Aluminum enhances inflammation and decreases mucosal healing in experimental colitis in mice. *Mucosal Immunol* 2014;7:589–601.
- [57] Stobaugh DJ, Deepak P, Ehrenpreis ED. Increased risk of osteoporosis-related fractures in patients with irritable bowel syndrome. *Osteoporos Int* 2013;24:1169–75.
- [58] Philippe C, Porter DE, Emerton ME, Wells DE, Simpson A, Monaco AP. Mutation screening of the EXT1 and EXT2 genes in patients with hereditary multiple exostoses. *Am J Hum Genet* 1997;61:520–8.